PHYSICAL REVIEW B **83**, 140406(R) (2011)

Short-range correlations and their thermal hysteresis in the paramagnetic phase of $YFe_3(BO_3)_4$

L. Rebbouh,[1] R. D. Desautels,[1] C. Ritter,[2] J. M. Cadogan,[1] V. Temerov,[3] A. Pankrats,[3] and J. van Lierop[1]
[1]*Department of Physics and Astronomy, University of Manitoba, Winnipeg, Manitoba, Canada R3T 2N2*
[2]*Institut Laue-Langevin, Boite Postale 156, F-38042 Grenoble, France*
[3]*L. V. Kirenskii Institute of Physics, Siberian Branch of RAS, Krasnoyarsk 660036, Russia*
(Received 9 February 2011; published 14 April 2011)

Neutron diffraction and Mössbauer spectroscopy have been used to examine the connections between long- and short-range magnetic order in the rare-earth iron ferroborate $YFe_3(BO_3)_4$. We establish the presence of short-range magnetic order in the pseudo-one-dimensional Fe-spin chains of the FeO_6 octahedra while the ferroborates are in their (long-range) paramagnetic phase. The short-range order exists at temperatures several times the Néel temperature. In addition, we observe thermal hysteresis of the short-range ordered Fe spins. The observed Fe-spin dynamics are suggestive of the presence of solitons within the domains that form in the Fe-spin chains.

DOI: 10.1103/PhysRevB.83.140406 PACS number(s): 76.75.+i, 75.50.Lk, 75.50.Tt

The recent introduction of the rare-earth ferroborates $GdFe_3(BO_3)_4$, $NdFe_3(BO_3)_4$,[1] and $HoFe_3(BO_3)_4$[2] into the family of multiferroics has rekindled interest in understanding the physics driving the complex structural, electric, and magnetic behavior of $RFe_3(BO_3)_4$, where R is a rare-earth ion or Yttrium. The magnetism in $RFe_3(BO_3)_4$ is particularly puzzling, due largely to the subtle interplay of the magnetic ground states of the $3d$ and $4f$ ions that exhibit different magnetic transitions with magnetic structures driven by competing anisotropies. While the R = Nd and Pr ferroborate structures retain a $R32$ phase down to the lowest temperatures, a structural transition from $R32$ to $P3_121$ occurs for R = Eu to Yb and Y between 90 and 450 K[3] (depending on the R^{3+} size) and the Er ferroborate stays in the $P3_132$ phase at temperatures up to ∼550 K.[4] In the $R32$ phase, edge-sharing FeO_6 octahedra form spiral chains running along the c axis where each R^{3+} ion is surrounded by six O^{2-} ions, forming triangular RO_6 prisms separated from one another by BO_3 triangles with no common O^{2-} ions. The distance between Fe^{3+} ions along the chains is considerably shorter than that between neighboring chains, adding a one-dimensional flavor to the magnetism. In the low-symmetry $P3_121$ phase there are two different Fe sites that lead to slightly different Fe–Fe distances along the spiral chains.[5] In addition, the R^{3+} ions are well separated from each other with no direct R–O–R (super)exchange. Interestingly, while the intrachain Fe–O–Fe interaction pathway may seem the most direct, Fe–O–B–O–Fe and Fe–O–R–O–Fe superexchange drives the second-order antiferromagnetic (AF) transition[6,7] $T_{N\mathrm{Fe}}$ in the 30–40 K range. This staggered magnetic field from the ordered Fe^{3+} ions polarizes the R^{3+} ions, driving them toward their own T_{NR} so that T_{NR}=$T_{N\mathrm{Fe}}$. Finally, the competition of the Fe and R contributions to the total magnetic anisotropy can also drive a spontaneous spin reorientation transition T_{SR} at temperatures below about 10 K[8–11] [e.g., T_{SR}= 5 K in $HoFe_3(BO_3)_4$[8]].

While the basic structural and magnetic properties of the $RFe_3(BO_3)_4$ system have become well established recently, understanding the exotic magnetism suggested by the low dimensionality of the Fe^{3+} ions together with the presence of their two coupled sublattices in the $P3_121$ phase and the R^{3+} ions has been a challenge. Raman scattering experiments provided some fascinating hints of the presence of short-range correlations in the paramagnetic phase of $GdFe_3(BO_3)_4$ and $NdFe_3(BO_3)_4$.[12] The spectral shape of the quasielastic scattering in the paramagnetic phase was well described by the response function of interacting magnons in low-dimensional quantum spin systems. Very recently neutron diffraction and polarimetry experiments on $NdFe_3(BO_3)_4$ demonstrated the existence of unequally populated domains with different "handedness" of the long-range AF order with domain lengths of ∼100 nm, with evidence of reduced Fe^{3+} moment sizes that were attributed to frustration effects,[13] arguing that atomic-level disorder was present that could be due to magnetic relaxation of some of the Fe^{3+}. Furthermore, above T_{SR} there was an indication of the presence of magnetic solitons[13] (moving domain walls that have been observed in quasi-one-dimensional antiferromagnets[14]) without the application of an external field, which is highly unusual. Most recently, hard x-ray scattering experiments on R = Nd and Gd ferroborates have provided compelling evidence of magnetic domains ∼10 nm in length.[15] The significant difference in domain wall lengths between techniques that both measure long-range magnetic order is perplexing.

To clarify the connections between the short- and long-range magnetism in $YFe_3(BO_3)_4$ and explore possible dynamics in the rare-earth ferroborates, we carried out neutron diffraction and susceptometry experiments to characterize the long-range magnetism, and we complemented these results with transmission Mössbauer spectroscopy that explores the short-range local magnetism. We show that there is a plethora of magnetic behavior above the long-range ordering temperature T_N of the rare-earth ferroborates. For example, the Fe^{3+} ions experience short-range order at temperatures at least twice T_N, whereupon the Fe spins fluctuate too rapidly to be measured in the "time window" of the ^{57}Fe Mössbauer transition. The Mössbauer spectra are well described using a simple magnetic relaxation model that incorporates the Kramers Fe^{3+} electronic magnetism[16] and relaxation rates of the Fe spins above T_N exhibit an exponential temperature dependence, indicative of nonlinear excitations in the (pseudo) one–dimensional Fe chains, for example, magnetic solitons.[14] Unexpectedly we found that repeated heating and cooling cycles while in the $P3_121$ phase resulted in short-range hysteretic behavior, indicating the domains were depinning and repinning into new configurations. Heating a rare-earth ferroborate through the $R32$ phase transition resets the system

so that the initial atomic magnetism was recovered in the $P3_121$ phase.

Single crystals of $RFe_3(BO_3)_4$ (R = Y, Ho, and Tb) were grown[6] and ground into powders. Superconducting quantum interference device (SQUID) susceptometry was performed with a quantum design Magnetic Properties Measurement System (MPMS) and neutron diffraction data were taken on the high-resolution powder diffractometer (D1A) and high-flux powder diffractometer (D1B) at the Institut Laue-Langevin in Grenoble. Mössbauer measurements were made in constant acceleration mode with a 1 GBq ^{57}Co**Rh** source. The spectrometer was calibrated using α-Fe at room temperature. Spectra were collected at temperatures ranging from 5 to 100 K in a Janis SHI-850 closed cycle refrigerator. Similar magnetism (long and short range) was observed in all three systems, with small differences in the temperature dependences of the hyperfine parameters due to the local field provided by the R^{3+} ions, so we shall limit the discussion in this paper to $YFe_3(BO_3)_4$, with a longer report on the R = Ho and Tb compounds forthcoming.

The temperature dependence of the magnetic susceptibility ($\chi = M/\mu_0 H$), together with $d\chi/dT$ that tracks with the specific heat's temperature dependence[17] shown in Fig. 1, are in agreement with previous measurements on $YFe_3(BO_3)_4$,[3] yielding $T_N = 37 \pm 2$ K. The inverse magnetic susceptibility's ($1/\chi = \mu_0 H/M$) temperature dependence (inset in the top panel of Fig. 1) with a Curie-Weiss law fit of the high-temperature data (shown by the solid line) reveal some small deviations from the Curie–Weiss law behavior around 40–45 K that may indicate the onset of short-range correlations. The results of neutron diffraction thermal scans (Fig. 1, bottom) after the system was cooled from the $R32$ phase into the $P3_121$ phase in a "virgin" state, and scans with the system always in the $P3_121$ phase clearly show that the long-range magnetism is unaltered and well described by a $J = 5/2$ Brillouin function (solid line) where $T_N = 37 \pm 1$ K.[10] These results are characteristic of the rare-earth ferroborate's long-range magnetism.

The results of transmission Mössbauer experiments over the same range of temperatures reveal quite different magnetism. In $YFe_3(BO_3)_4$ we observed at 5 K a well resolved six-line spectrum (Fig. 2 left) which shows that the Fe atoms in the Fe^{3+} chains are fully ordered magnetically. This result is expected at temperatures well below T_N. Upon warming there is a small decrease in the spectral line positions (e.g., 30 K spectrum in Fig. 2 left) that signifies a smaller hyperfine field ($B_{\rm hf}$) which is proportional to the Fe moment. The ~6% decrease in $B_{\rm hf}$ from 5 to 30 K (see below) is in good agreement with the decrease in the Fe moment measured by neutron diffraction (Fig. 1); to this point the short-range magnetism has tracked with the long-range magnetism. The first surprise that the spectra held occurred at temperatures above T_N. To begin, we consider the spectrum collected at 50 K (35% above T_N), where the spatially and temporally averaged magnetization of the Fe^{3+} chains should be zero. Recall that neutron diffraction and dc susceptibility measurements ascertain the same T_N and have very different measuring time scales (e.g., 10^{-12}–10^{-13} s for neutrons, and 0.5–1 s per measurement for the SQUID magnetometry). If dynamical freezing were present instead of a magnetic phases transition from an antiferromagnetic to paramagnetic state, one would expect very different temperatures

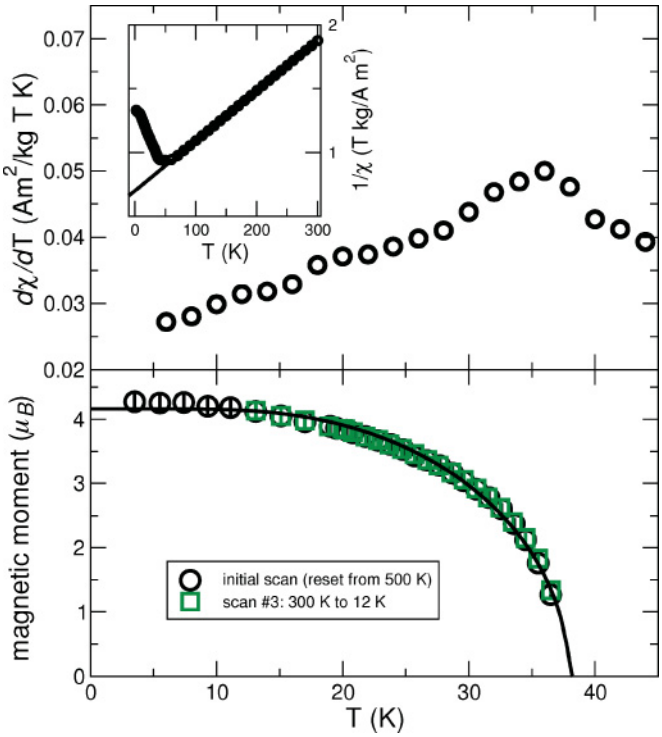

FIG. 1. (Color online) Top: Fisher plot[17] (temperature derivative of the dc susceptibility χ) of $YFe_3(BO_3)_4$ where the peak, upon warming, denotes the onset of short-range magnetic correlations in an AF. The inset shows the temperature dependence of the low field (0.01 T) inverse susceptibility ($1/\chi$) over the complete range of temperatures with the solid line a Curie–Weiss law fit. Bottom: The temperature dependence of the average Fe moment from neutron diffraction data, with ○ the moment's value after cooling from the $R32$ to the $P3_121$ phase and □ the moment's value after two previous scans from 300 to 12 K. All measurements yield $T_N \sim 37$ K.

where zero measured magnetization and moment occurred. The Mössbauer effect time scale is around 10^{-6} s, intermediate between neutron and magnetometry techniques; however it is sensitive to atomic level, short-range magnetism while neutrons and magnetometry probe the long-range magnetism (magnetic order). The 50 K spectrum in Fig. 2 show that while the spectral line shape has changed considerably, with broadened lines and a change in the relative intensity of the six lines, the presence of the six-line spectrum shows undeniably that Fe^{3+} ions in the chains must be experiencing short-range magnetic order. Indeed, $B_{\rm hf}$ is reduced further from its 30 K value (spectral line positions are collapsing to lower velocities and energies) at 50 K, but only by 70 K (Fig. 2 left) is the local, time-averaged hyperfine field reduced to zero, resulting in a single spectral line being observed. These spectra provide clear, direct evidence of short-range magnetic correlations in the rare-earth ferroborates in their paramagnetic state.

After obtaining the thermal evolution of the spectra that were collected upon cooling *after* the rare-earth ferroborate has been warmed above T_N, we collected spectra after the system had been cooled from 300 K (each time) at temperatures between 5 and 70 K. As shown in the right panel of Fig. 2, repeated cooling scans from 300 to 45 K resulted in readily observable spectral differences with, for example, a reduced

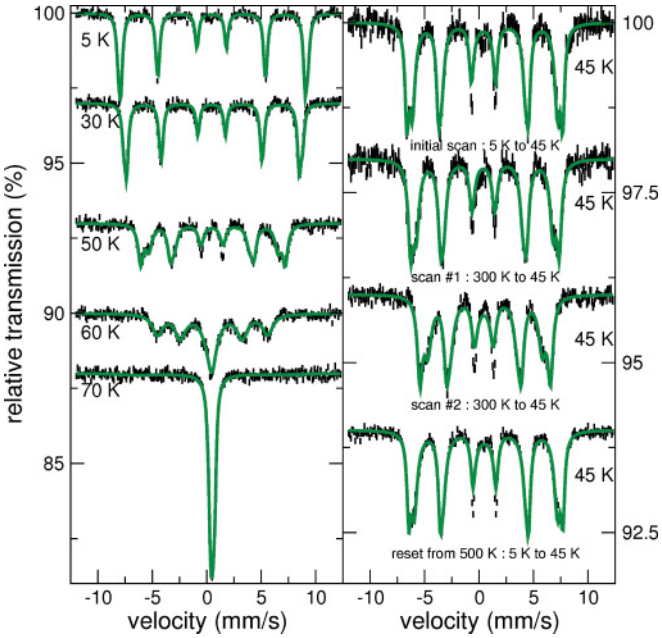

FIG. 2. (Color online) Left: Typical Mössbauer spectra of $YFe_3(BO_3)_4$ with the system in its virgin state after being cooled from the $R32$ phase. Right: Mössbauer spectra after the initial cool down from the $R32$ phase at 45 K (top), with the results at 45 K of two thermal scans from 300 K (middle) showing clearly the effects of thermal hysteresis, and a return to the initial magnetic state after being "reset" at 500 K from the $R32$ into the $P3_121$ phase at 45 K (bottom). The solid lines are fits described in the text.

$B_{\rm hf}$ between the initial cool down from 5 to 45 K and cooling from 300 to 45 K several more times. Clearly, the short-range magnetic order (recall that 45 K is well into the paramagnetic phase) experiences thermal hysteresis. The short-range magnetism cooled from 300 K to temperatures below T_N revealed a weaker yet distinct hysteresis. No sign of thermal hysteresis was detectable in the long-range magnetism (Fig. 1) by neutron diffraction where the system underwent similar thermal cycling. When the system was heated to 500 K (in an Ar gas atmosphere) which reintroduced the $R32$ to $P3_121$ structural phase transition upon cooling, the original short-range magnetism was recovered, as shown by the identical spectra at 45 K from the initial thermal scan from 5 to 45 K (top spectrum in the right panel of Fig. 2) and the 5 to 45 K scan after the sample was reset from 500 K (bottom spectrum in the right panel of Fig. 2). These results illustrate the strong interrelationship between the structural and short-range magnetic properties in the rare-earth ferroborates most clearly; trends that have been suggested by previous studies.[12,13,15]

An appropriate line shape model to quantify the trends presented by the spectra needed to conform to the magnetic structure identified by neutron diffraction[10] and the Kramers character of the Fe^{3+} chain ions. These constraints and the ability to fit the spectra over the complete range of temperatures consistently called for the spin-relaxation model of Wickman and Wertheim.[16] The model essentially combined a two-level magnetic relaxation formalism with ionic-Zeeman splitting of two different (uniaxially symmetric) electronic configurations described by an effective Hamiltonian, $\mathcal{H} = g\mu_B H I_z + A_z S_z I_z$.[18] H is the effective field at the ^{57}Fe nucleus, A_z is the energy splitting associated with the Kramers doublet, $I_z = \pm 1/2, 3/2$ and $S_z = \pm 1/2$, with the probabilities of occupying either of the Kramers states being $\exp(\Delta/k_BT)$ and $[1 - \exp(\Delta/k_BT)]$. This model, combined with the hyperfine parameters for ^{57}Fe (e.g., hyperfine field $B_{\rm hf}$, isomer shift IS, and quadrupole shift QS) and line intensities proportional to the appropriate Clebsch-Gordon coefficients, permitted us to fit the Mössbauer spectra successfully. We note that neither simpler magnetic relaxation models[19] nor line shape calculations incorporating distributions of electric and magnetic environments[20] were able to describe the thermal evolution of the spectra consistently.

The spectra were fitted with two sites, where the lowest temperature spectra (5 K) were used to determine the static hyperfine parameters, such as linewidth (Γ) the isomer shift IS, and quadrupole shift QS. The relative absorption of the two sites fitted to 0.33 ± 0.05 and 0.67 ± 0.07 in excellent agreement with the magnetic structure determined from neutron diffraction experiments[10] where 1/3 of the Fe reside in the 3a sites and 2/3 in the 6c sites. $IS = 0.513 \pm 0.009$ mm/s and $QS = -0.025 \pm 0.003$ mm/s for the 3a site, while $IS = 0.507 \pm 0.005$ mm/s and $QS = -0.020 \pm 001$ mm/s for the 6c site. These results show that while the electron densities are the same at the ^{57}Fe nuclei (in the Fe chains) at the two sites, the electric field gradients were slightly different, in accord with the 6c Fe sites having closer B neighbors. $\Gamma = 0.152 \pm 0.007$ mm/s FWHM was required to fit the spectra, slightly broadened compared to the source's natural linewidth of 0.135 ± 0.005 mm/s, reflecting a small amount of chemical disorder that resulted in a small distribution of nuclear environments about the ^{57}Fe atoms.

The temperature dependences of the fitted $B_{\rm hf}$, Δ, and ν (relaxation rate between $I_e \rightarrow I_g$ states) for the 3a and 6c sites are shown in Fig. 3. Typically, $B_{\rm hf}$ and ν are correlated strongly since ν describes the collapse of spectral line positions toward zero (e.g., a time-averaged hyperfine field) that can be approximated with a reduced $B_{\rm hf}$. However $\nu(T)$ also reflects changes in line shape that cannot be dealt with by a $B_{\rm hf}(T)$ correctly, and the measured variations in line shape with temperature (Fig. 2) were distinct enough to virtually decouple correlations between $B_{\rm hf}$, ν, and Δ up to the highest temperatures (>55 K). At those temperatures no sextet component was resolvable and $B_{\rm hf}$ was fixed at its lower temperature value.

The results of thermal scans when the $YFe_3(BO_3)_4$ was in its virgin state, having just been cooled through the $R32$ to $P3_121$ phase transition, are described by scans zero and four (four being from a thermal reset as described previously), while scans one through three are when the system was cycled thermally in the $P3_121$ phase. As shown in Fig. 3, at temperatures up to T_N, $B_{\rm hf}(T)$ tracked well with the long range Fe^{3+} moment's temperature dependence as determined by neutron diffraction (Fig. 1). The values of $B_{\rm hf}$ are consistent with Fe^{3+}, however we point out that determining a moment value for the Fe sites from Mössbauer results for direct comparison to the values shown in Fig. 1 is problematic due to local orbital and crystal field effects. The results of the thermal scans where the system was heated to 300 K before the measurement revealed the first hints of a hysteretic process via a small reduction of $B_{\rm hf}(T)$ above ~20 K with warming compared to the initial thermal scan (scan zero) values.

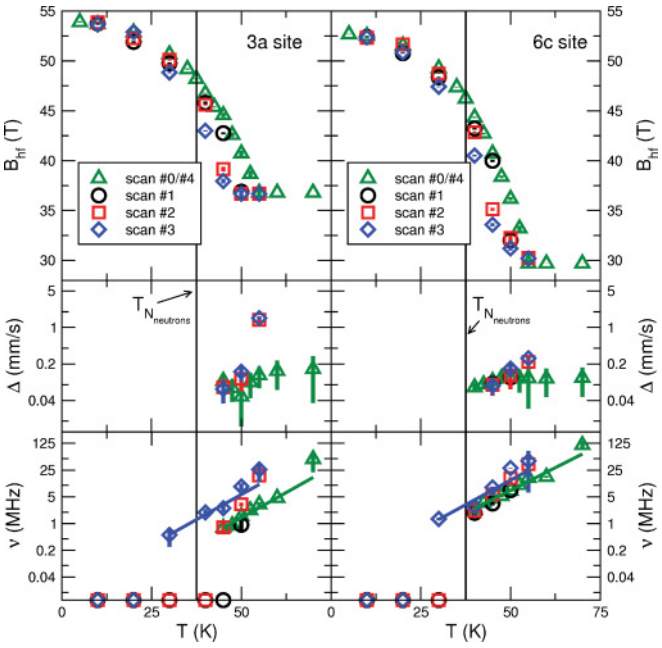

FIG. 3. (Color online) Temperature dependence of the fitted hyperfine parameters for the 3a and 6c sites in $YFe_3(BO_3)_4$ where B_{hf} are the hyperfine fields, Δ is the ground Kramers doublet energy, and (ν) is the relaxation rates of ^{57}Fe atoms between the I_g and I_e states (note that ν is plotted on a log–linear scale). The solid lines are fits described in the text.

For temperatures above T_N, where the long-range antiferromagnetic order is no longer present, the short-range Fe-chain magnetism becomes intriguing. Above T_N the fits require $\Delta>0$; crystal field effects are no longer suppressed and the Fe^{3+} ions fluctuate slowly between the hyperfine environments of the two-fold degenerate states, whose energy remains essentially constant with temperature ($\Delta\sim0.1$ mm/s $\equiv$ 0.2 mK, Fig. 3). Simultaneously, B_{hf} of the two Fe sites continued their monotonic decrease with warming until ∼50 K, whereupon the Fe spins were fluctuating too quickly to decouple static and magnetic relaxation effects. Thermal scans exploring the hysteresis showed that the local crystal fields were only weakly affected. However, $B_{hf}(T)$ of the 3a and 6c sites decreased with successive thermal cycles, indicating that the exchange interactions driving the short-range magnetic ordering were weakening (Fig. 3).

The exponential temperature dependence of ν in Fig. 3 (shown by the solid lines) corroborates the polarized neutron studies that indicated the presence of magnetic solitons. Using the classical sine-Gordon description of nonlinear excitations, the flip rate for the electronic spins above the magnetic ordering temperature in a magnetic soliton (for low domain wall densities) is $\nu(T) \propto \exp(-E_b/k_BT)$ where E_b represents the creation energy of a magnon bound state.[14] The slowing of ν with cooling can be attributed to the progressive blocking of wall propagation. $E_b = 0.25\pm0.01$ K from the Mössbauer experiments (scan zero). E_b from $\nu(T)$ decreased from 0.25 to 0.18 ± 0.02 K (scan 3) with repeated heating and cooling cycles in the $P3_121$ phase. Since $E_b\simeq2J_z$ where J_z is the exchange energy between spins in the soliton,[14] this observed reduction in J_z tracks well with the indications of weakening exchange from $B_{hf}(T)$ described above. Alternatively, the changes in E_b may be from smaller domain walls surviving after depinning during thermal cycling, resulting in fewer Fe–Fe exchange interactions being reflected with a smaller $B_{hf}(T)$. Indeed, this interpretation could explain the different domain wall lengths determined from neutron and x-ray measurements.[13,15]

This work was supported by grants from the Natural Sciences and Engineering Research Council of Canada and the Canada Foundation for Innovation. J.M.C. acknowledges support from the Canada Research Chairs program.

[1] A. Zvezdin, S. S. Krotov, A. M. Kadomtseva *et al.*, JETP Lett. **81**, 272 (2005); A. K. Zvezdin, G. P. Vorob'ev, A. M. Kadomtseve *et al.*, *ibid.*, **83**, 509 (2006).

[2] R. P. Chaudhury, F. Yen, B. Lorenz, Y. Y. Sun, L. N. Bezmaternykh, V. L. Temerov, and C. W. Chu, Phys. Rev. B **80**, 104424 (2009).

[3] Y. Hinatsu, Y. Doi, K. Ito, M. Wakeshima, and A. Alemi, J. Solid State Chem. **172**, 438 (2003).

[4] C. Ritter, A. Vovotynov, A. Pankrats *et al.*, J. Phys. Condens. Matter **22**, 206002 (2010).

[5] S. A. Klimin, D. Fausti, A. Meetsma *et al.*, Acta Crystallogr. Sect. B **61**, 481 (2005).

[6] C. Ritter, A. D. Balaev, A. Vorotynov *et al.*, J. Phys. Condens. Matter **19**, 196227 (2007).

[7] A. I. Pankrats, G. A. Petrakovskii, L. N. Bezmaternykh *et al.*, Phys. Solid State **50**, 79 (2008).

[8] A. D. Balaev, L. N. Bezmaternykh, I. A. Gudim *et al.*, J. Magn. Magn. Mater. **258/259**, 532 (2003); E. A. Popova, D. V. Volkov, A. N. Vasiliev *et al.*, Phys. Rev. B **75**, 224413 (2007).

[9] A. I. Pankrats, G. A. Petrakovskii, L. N. Bezmaternykh *et al.*, JETP **99**, 766 (2004).

[10] C. Ritter, A. Vovotynov, A. Pankrats *et al.*, J. Phys. Condens. Matter **20**, 365209 (2008).

[11] A. Pankrats, G. Petakovskii, A. Kartashev *et al.*, J. Phys. Condens. Matter **21**, 436001 (2009).

[12] D. Fausti, A. A. Nugroho, P. H. M. van Loosdrecht, S. A. Klimin, M. N. Popova, and L. N. Bezmaternykh, Phys. Rev. B **74**, 024403 (2006).

[13] M. Janoschek, P. Fischer, J. Schefer, B. Roessli, V. Pomjakushin, M. Meven, V. Petricek, G. Petrakovskii, and L. Bezmaternikh, Phys. Rev. B **81**, 094429 (2010).

[14] H. J. M. de Groot, L. J. de Jongh, R. C. Thiel, and J. Reedijk, Phys. Rev. B **30**, 4041 (1984).

[15] J. E. Hamann-Borrero, M. Philipp, O. Kataeva, M. v. Zimmermann, J. Geck, R. Klingeler, A. Vasiliev, L. Bezmaternykh, B. Buchner, and C. Hess, Phys. Rev. B **82**, 094411 (2010).

[16] H. H. Wickman and G. K. Wertheim, in *Chemical Applications of Mössbauer Spectroscopy*, edited by V. I. Goldanskii and R. H. Herber (Academic, New York, 1968).

[17] M. E. Fisher, Philos. Mag. **7**, 1731 (1962).

[18] I. Nowik and H. H. Wickman, Phys. Rev. Lett. **17**, 949 (1966).

[19] M. Blume and J. A. Tjon, Phys. Rev. **165**, 446 (1968).

[20] G. Le Caër and J. M. Dubois, J. Phys. E **12**, 1083 (1979).